A Stranger in a Strange Fractional Land

J. Tenreiro Machado

ISEP, Portugal

Oct 2016

A Stranger in a Strange Land

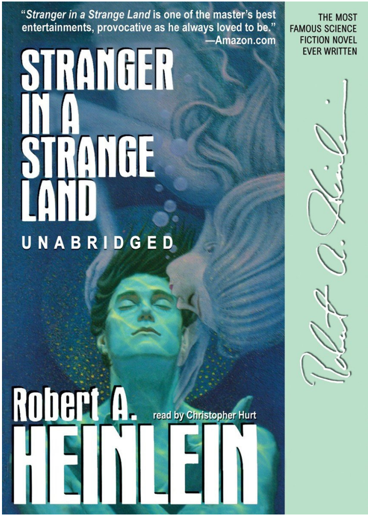

- The title is inspired by the famous 1961 science fiction novel entitled "Stranger in a Strange Land" by American writer Robert A. Heinlein
- The story focuses on a human raised on Mars and his adaptation to, and understanding of, humans and their culture.

Fractional Calculus: From "strange" to popular topic

- J. Machado, V. Kiryakova, F. Mainardi, Recent History of Fractional Calculus, CNSNS, vol. 16, 3, 1140-1153, 2011
- J. Machado, A. Galhano, J. Trujillo, Science Metrics on Fractional Calculus Development Since 1966, FCAA, vol. 16, 2, 479-500, 2013
- J. Machado, A. Galhano, J. Trujillo, On Development of Fractional Calculus During the Last Fifty Years, Scientometrics, vol. 98, 1, 577-582, 2014

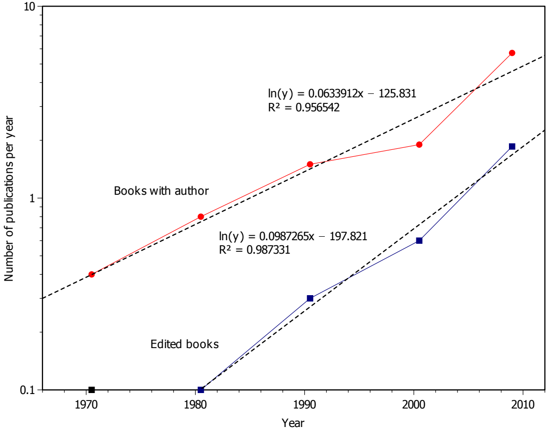

"Where Do We Come From? What Are We? Where Are We Going?", Paul Gauguin

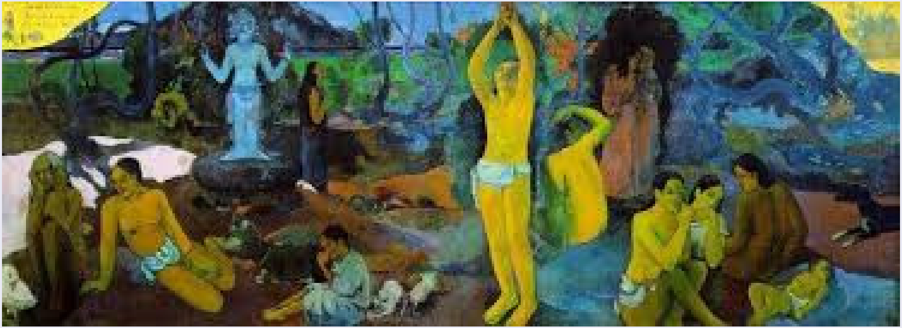

Development of FC

Present day popular directions of progress are:

- new definitions of operators and "fractionalization" of models
- in-depth study of some mathematical formulations.

Pros and cons

- The first may lead to fast advances and open research new topics, but can produce possible misleading or even erroneous formulations
- The second, constitutes a solid basis, but its limited scope narrows the horizons of FC to a limited number of topics and produces slower advances

Progress in Education

- Investment in FC education
- Mixing FC with classical topics

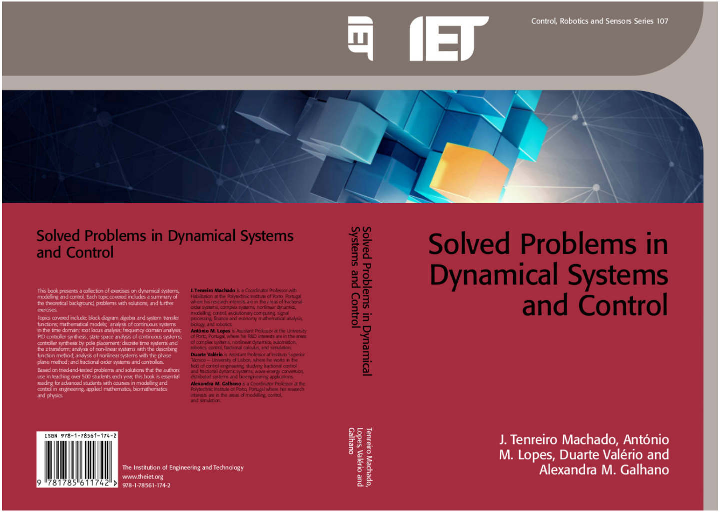

Albert Einstein: Imagination

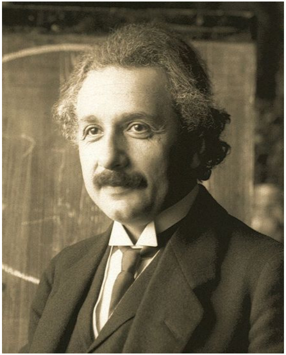

Imagination is more important than knowledge. For knowledge is limited, whereas imagination embraces the entire world, stimulating progress, giving birth to evolution.

The strange research in the strange topic

Possible new directions of progress in FC may emerge in the fringe of classical science, or in the borders between two or more distinct areas.

The paradox

We should have in mind that some of those strange fractional objects "will lead to a paradox, from which one day useful consequences will be drawn"

The Event

Workshop on Future Directions in Fractional Calculus Research and Applications

Portuguese discoveries: 15th and 16th centuries

The age of discoveries, fueled by the rise of the "dynamic thinkers" of the new Portugal, started with the Kingdom of Dom Joao I

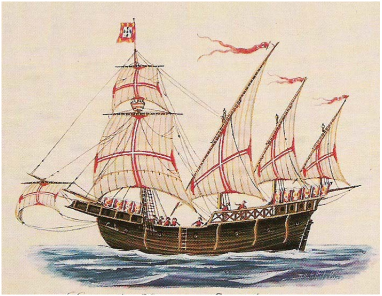

StarTrek's monologue

"... to explore strange new worlds, to seek out new life and new civilizations, to boldly go where no man has gone before."

Fractional objects

- Generalized junctions
- Generalized two-port elements
- Matrix fractional systems
- Generalization of memristor and higher order elements
- Generalized information
- Visualization of dynamics
- Modeling vegetables
- Analyzing terrorism

Fractional object: Generalized junctions

J. A. Tenreiro Machado, Fractional Order Junctions, Communications in Nonlinear Science and Numerical Simulation, vol. 20, Issue 1, pp. 1-8, 2015

Generalized junctions

- The Kirchhoff's first and second laws constitute the so-called parallel and series junctions in the scope of network methods.
- The Kirchhoff's current and voltage laws (KCL, KVL) represent the principles of conservation of electric charge and conservation of flux.
- These junctions establish simple algebraic restrictions in a network.
- The sums of directed currents i, in conductors meeting at a point, or of voltages v, in any closed loop, are zero:

$$\text{KCL: } \sum_k i_k = 0, \ \text{KVL: } \sum_k v_k = 0. \tag{1}$$

We consider the interconnection of an α-inductor with value L and a β-capacitor with value C

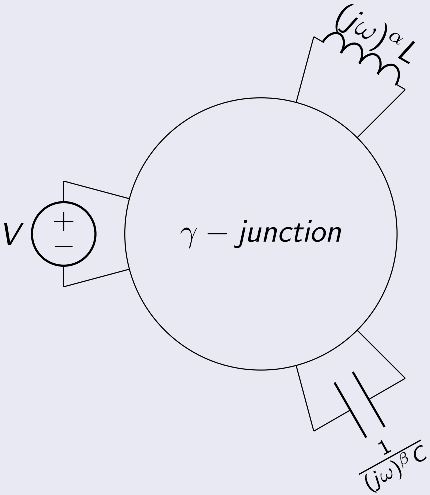

The γ-junction establishes the dynamic relationship:

$$\left\langle \frac{1}{2}\left\{ \left[(j\omega)^{\alpha} L\right]^{\gamma} + \left[\frac{1}{(j\omega)^{\beta} C}\right]^{\gamma} \right\} \right\rangle^{\frac{1}{\gamma}} = Z(j\omega)\,,\ \gamma \neq 0, \qquad (2a)$$

$$(j\omega)^{\frac{\alpha-\beta}{2}} \sqrt{\frac{L}{C}} = Z(j\omega)\,,\ \gamma = 0, \qquad (2b)$$

- For $\gamma = -1$ and $\gamma = 1$, expression (21) reduces to the parallel and series junctions of two elements.
- For $\gamma = 0$ we get a single element with impedance $Z(j\omega) = (j\omega)^{\frac{\alpha-\beta}{2}} \sqrt{\frac{L}{C}}$

Let us consider the voltage source $v(t) = \sin(\pi t)\,,\ -1 \leq t \leq 1,$

The Fig. shows the final energy $e(t=1)$ for $-8 \leq \gamma \leq 8$ and the integer-order elements $j\omega L$ and $\frac{1}{j\omega C}$ ($L = 1,\ C = 1$). It is interesting to note that we have dissipative junctions for most values of γ and that the energy conservative cases are “rare”. The conservative cases occur not only for odd values of γ, but also a set of symmetrical values that evolve asymptotically as a power of $\frac{1}{2}$. The “oscillating” behaviour of the chart tends to stabilize its structure for large positives of γ.

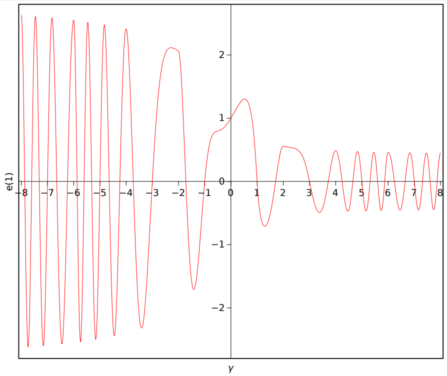

Fractional object: Generalized two-port elements

J. Tenreiro Machado, Alexandra M. Galhano, Generalized two-port elements, Communications in Nonlinear Science and Numerical Simulation, vol. 42, pp. 451-455, 2017.

Generalized two-port elements

The fractional α-inductor L, $0 < \alpha < 1$, and the fractional β-capacitor C, $0 < \beta < 1$, have impedances:

$$Z(j\omega) = (j\omega)^{\alpha} L, \; Z(j\omega) = \frac{1}{(j\omega)^{\beta} C}. \tag{3}$$

Often these "fractor" elements are also denoted as "fractductor" and "fractance" with the following symbols.

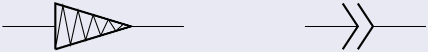

Classical two-port elements

The transformer (TF) and the gyrator (GY) are two-port networks relating the voltages and currents at the primary, v_1 and i_1, with the voltages and currents at the secondary circuit, v_2 and i_2, by means of the equations

$$TF: \; v_1(t) = k \cdot v_2,(t), \; i_1(t) = k^{-1} \cdot i_2(t), \tag{4a}$$

$$GY: \; v_1(t) = k \cdot i_2(t), \; i_1(t) = k^{-1} \cdot v_2(t), \tag{4b}$$

where k (dimensionless for the TF and in Ω for the GY) are denoted as the transformation and gyration ratios.

Classical two-port elements

The relations in (15) for the TF and the GY can be directly transformed into the Fourier domain and we can write instead:

$$TF: \; V_1(j\omega) = k \cdot V_2,(j\omega), \; I_1(j\omega) = k^{-1} \cdot I_2(j\omega), \tag{5a}$$

$$GY: \; V_1(j\omega) = k \cdot I_2(j\omega), \; I_1(j\omega) = k^{-1} \cdot V_2(j\omega), \tag{5b}$$

where $\mathcal{F}\{v_1(t)\} = V_1(j\omega)$, $\mathcal{F}\{v_2(t)\} = V_2(j\omega)$, $\mathcal{F}\{i_1(t)\} = I_1(j\omega)$ and $\mathcal{F}\{i_2(t)\} = I_2(j\omega)$.

Generalized two-port elements

The classical TF and GY can be interpreted as two-port elements of integer-order and, consequently, conceive their generalization toward fractional-orders.

The model for the TF and the GY in the Fourier domain can be interpreted as special cases of:

$$V_1\left(j\omega\right) = k \cdot V_2^{\theta}\left(j\omega\right) I_2^{1-\theta}\left(j\omega\right) \tag{6a}$$

$$I_1\left(j\omega\right) = k^{-1} V_2^{1-\theta}\left(j\omega\right) I_2^{\theta}\left(j\omega\right), \tag{6b}$$

where $\theta \in \mathbb{R}$ denotes the fractional order of the "generalized two-port element" (GTP).

Generalized two-port elements

In the time domain we have:

$$v_1(t) = k \cdot v_{2,\theta}(t) * i_{2,1-\theta}(t), \tag{7a}$$

$$i_1(t) = k^{-1} \cdot v_{2,1-\theta}(t) * i_{2,\theta}(t), \tag{7b}$$

where the symbol $*$ denotes the operation of convolution, $v_{2,\theta}(t) = \mathcal{F}^{-1}\left\{V_2^{\theta}(j\omega)\right\}$, $v_{2,1-\theta}(t) = \mathcal{F}^{-1}\left\{V_2^{1-\theta}(j\omega)\right\}$, $i_{2,\theta}(t) = \mathcal{F}^{-1}\left\{I_2^{\theta}(j\omega)\right\}$ and $i_{2,1-\theta}(t) = \mathcal{F}^{-1}\left\{I_2^{1-\theta}(j\omega)\right\}$.

Generalized two-port elements

The cases of $\theta = 1$ and $\theta = 0$ lead to the TF and GY, respectively. The standard symbols for the TF and GY are represented in the Fig. together with the proposed GTP.

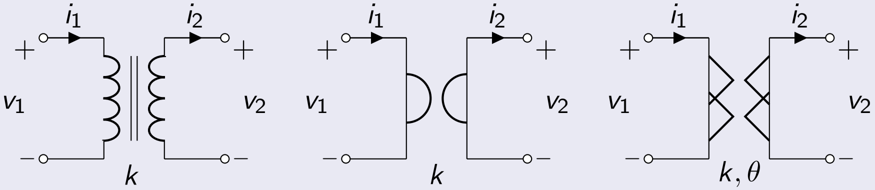

For an impedance $Z_2(j\omega)$ in the secondary, the impedance seen at the primary $Z_1(j\omega)$ is:

$$Z_1(j\omega) = \frac{V_1(j\omega)}{I_1(j\omega)} = k^2 Z_2^{2\theta-1}(j\omega). \tag{8}$$

In the simulation of the time response of fractional-order elements since we can take advantage of the GTP to obtain a fractor based on a integer-order impedance at the secondary.

For example, the Fig. shows the time response of $v_1(t)$ and $i_1(t)$ for an input square wave, a GTP with $k = 1$ and $\theta = 0.4$, and a capacitance at the secondary with $C = 1$.

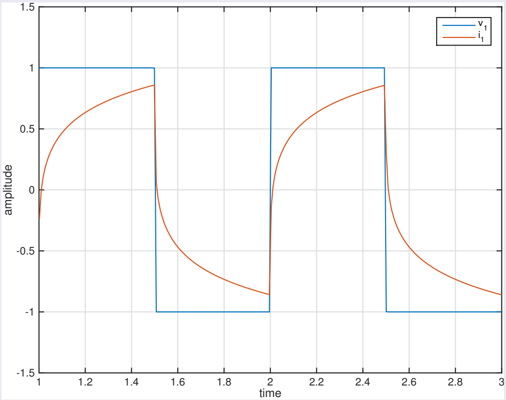

Fractional object: Matrix fractional systems

J. A. Tenreiro Machado, Matrix Fractional Systems, Communications in Nonlinear Science and Numerical Simulation, vol. 25, Issues 1-3, pp. 10-18, 2015.

Transfer functions (TF)

$$\text{Cole-Cole TF: } G(s) = \frac{K}{\left(\frac{s}{\omega_0}\right)^{\alpha} + 1}, \tag{9}$$

$$\text{Davidson-Cole TF: } G(s) = \frac{K}{\left(\frac{s}{\omega_0} + 1\right)^{\gamma}}, \tag{10}$$

$$\alpha = 1 \vee \gamma = 1 \Rightarrow \text{Debye TF: } G(s) = \frac{K}{\frac{s}{\omega_0} + 1}. \tag{11}$$

$$\text{Havriliak-Negami TF: } G(s) = \frac{K}{\left[\left(\frac{s}{\omega_0}\right)^{\alpha} + 1\right]^{\gamma}}. \tag{12}$$

Locus of Debye, Cole-Cole, Davidson-Cole, and Havriliak-Negami TF

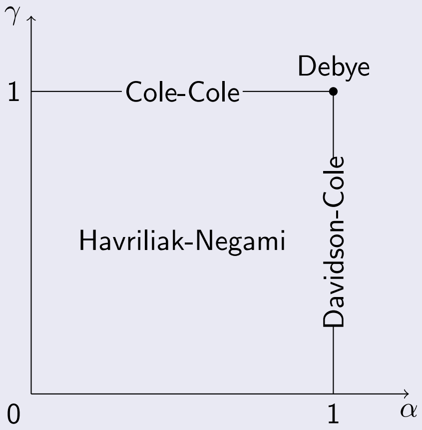

Generalization to multidimensional representation

We need to evaluate the TF matrix $\mathbf{Z}(s)$ for non-integer powers μ. One reliable method for computing $\mathbf{Z}^{\mu} = \mathbf{W}$ is based on the eigenvalue decomposition.

For a $n \times n$ matrix $\mathbf{Z}$, with eigenvalues λ_i and eigenvectors $\mathbf{v}_i \neq \mathbf{0}$, $i = 1, \cdots, n$, so that $\mathbf{Z}\mathbf{v}_i = \lambda_i \mathbf{v}_i$, there is the well know relation

$$\mathbf{Z}^{n}\mathbf{v}_i = \lambda_i^{n}\mathbf{v}_i,\ n \in \mathbb{N} \tag{13}$$

For $n = \frac{1}{p}$, $p \in \mathbb{Z}$, $p \neq 0$, expression (13), yields:

$$\mathbf{Z}^{\frac{1}{p}}\mathbf{v}_i = \lambda_i^{\frac{1}{p}}\mathbf{v}_i. \tag{14}$$

The p-th root of $\mathbf{Z}$ can be defined as matrix $\mathbf{W}$ such that $\mathbf{W}^{p} = \mathbf{Z}$.

Analysis of an Electrical Circuit

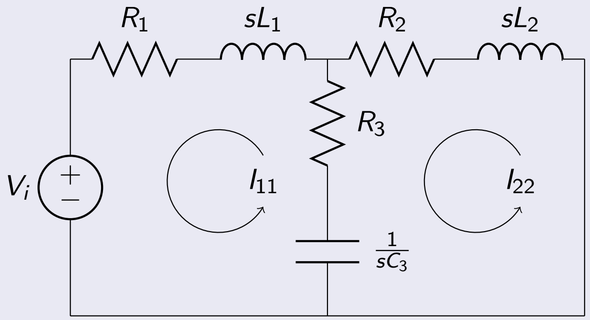

Circuit model using the mesh-current method

$$\mathbf{V} = \mathbf{ZI} : \begin{bmatrix} V_i \\ 0 \end{bmatrix} = \begin{bmatrix} R_1 + R_3 + sL_1 + \frac{1}{sC_3} & -R_3 - \frac{1}{sC_3} \\ -R_3 - \frac{1}{sC_3} & R_2 + R_3 + sL_2 + \frac{1}{sC_3} \end{bmatrix} \begin{bmatrix} I_{11} \\ I_{22} \end{bmatrix} \quad (15)$$

The corresponding fractional system is:

$$\mathbf{V} = \mathbf{Z}^{\mu}\mathbf{I}, \mu \in \mathbb{C}. \tag{16}$$

frequency response:
$R_1 = 1$,
$R_2 = 1$,
$R_3 = 1$,
$L_1 = 1$,
$L_2 = 1$,
$C_3 = 1$

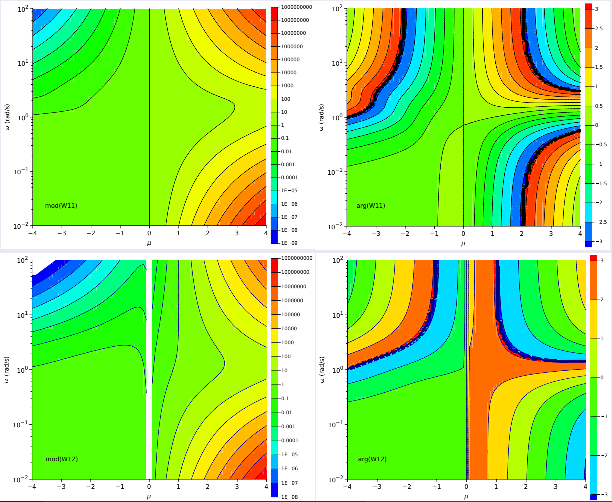

Circuit approximation

- The HN model has no direct implementation.
- We consider using integer and fractional elements.
- A compromise between simplicity and accuracy could be reached using:
  - series of one resistance and one "fractductor", and parallel with one "fractance", for $\mu = -0.5$
  - series of one "fractductor" and one "fractance", for $\mu = 0.5$.

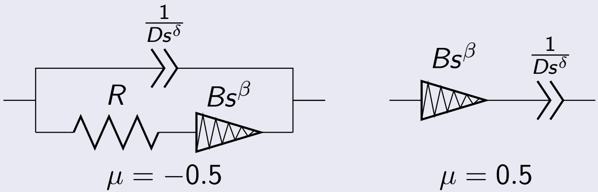

Fractional object: Generalization of memristor and higher order elements

J. A. Tenreiro Machado, Fractional Generalization of Memristor and Higher Order Elements, Communications in Nonlinear Science and Numerical Simulation, vol. 18, Issue 12, pp. 264-275, 2013.

Memristor

- In 1971 Leon Chua noticed the symmetry between electrical elements and variables and proposed the 4th element Memristor
- In 1980 Chua introduced the “Periodic table of all two-terminal elements”
- In 2012 Jeltsema and Dòria-Cerezo proposed higher order elements

Memristor and higher order elements

$$\text{inductor } L\text{:}\ \ v(t) = L\frac{di(t)}{dt} \tag{17}$$

$$\text{resistor } R\text{:}\ \ v(t) = Ri(t) \tag{18}$$

$$\text{capacitor } C\text{:}\ \ v(t) = \frac{1}{C}\int_{-\infty}^{t} i(\tau)\, d\tau \tag{19}$$

$$\text{magnetic flux:}\ \ \phi(t) = \int_{-\infty}^{t} v(\tau)\, d\tau \tag{20}$$

$$\text{electrical charge:}\ \ q(t) = \int_{-\infty}^{t} i(\tau)\, d\tau \tag{21}$$

The missing element: Memristor

$$\text{memristor } M\text{: } \phi(t) = Mq(t) \tag{22}$$

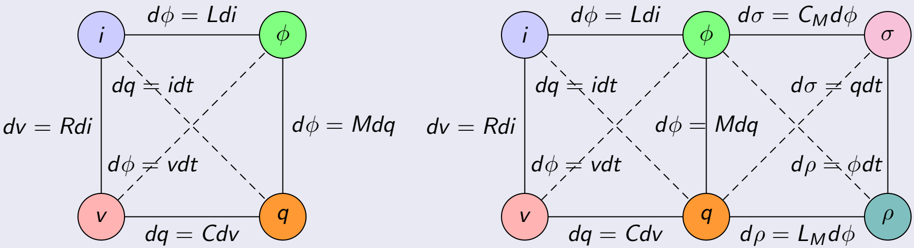

Periodic table of all two-terminal circuit elements

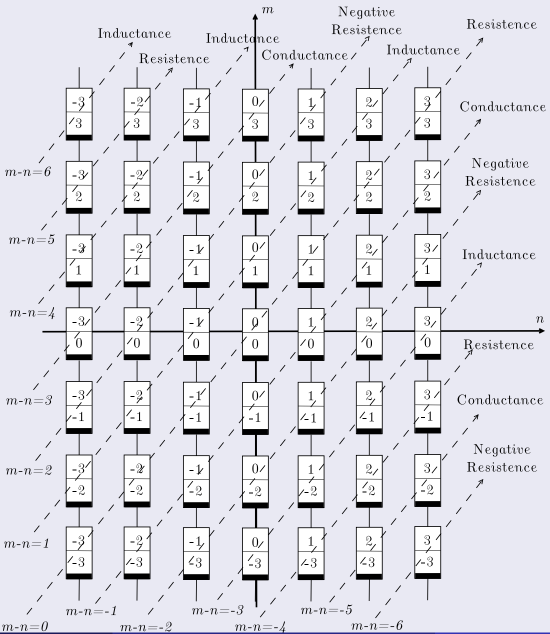

Integer and fractional order interpretation of circuit elements

- We can redraw the fundamental relationships: subdividing the first order integral I^1 as two fractional integrals I^α and $I^{1-\alpha}$
- The elements that involve energy storage/dissipation are indicated by the diagonal/vertical arrows.
- This means that the elements resistor and memristor have now a fractional order counterpart between the variables $I^\alpha i(t)$ and $I^\alpha v(t)$.

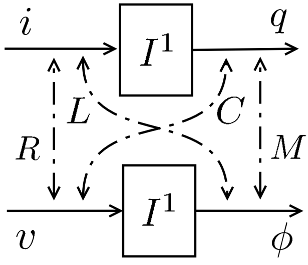

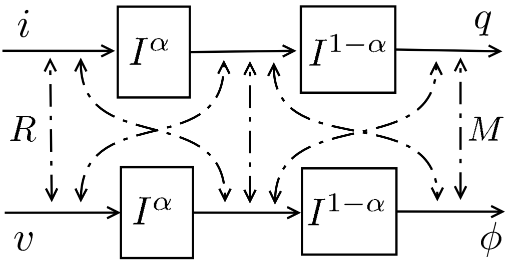

Generalized information

J. A. Tenreiro Machado, Fractional Order Generalized Information, Entropy vol. 16, no. 4, pp. 2350-2361, 2014

Shannon entropy

- The information content I of an event having probability of occurrence p_i is given by:
  $I\left(p_i\right) = -\ln p_i$
- The expected value of I, called Shannon entropy becomes:
  $S = E\left(-\ln p\right) = \sum_i (-\ln p_i) p_i,$
  where $E\left(\cdot\right)$ denotes the expected value operator

Entropy vs FC

The Shannon information $I(p_i) = -\ln p_i$ is a function between the cases:

- $D^{-1} I(p_i) = p_i (1 - \ln p_i)$
- $D^{0} I(p_i) = -\ln p_i$
- $D^{1} I(p_i) = -\frac{1}{p_i}$

FC Generalization

Information and entropy of order $\alpha \in \mathbb{R}$:

- $I_\alpha(p_i) = D^\alpha I(p_i) = -\frac{p_i^{-\alpha}}{\Gamma(\alpha+1)} [\ln p_i + \psi(1) - \psi(1-\alpha)]$
- $S_\alpha = \sum_i \left\{ -\frac{p_i^{-\alpha}}{\Gamma(\alpha+1)} [\ln p_i + \psi(1) - \psi(1-\alpha)] \right\} p_i,$

  where $\Gamma(\cdot)$ and $\psi(\cdot)$ represent the gamma and digamma functions.

Fractional Entropy

Two examples of applications:

- In the Dow Jones Industrial Average time series we have:
  - Daily values during the period May 18, 1987 - March 14, 2014.
  - A total of $L = 7000$ data values
  - For the calculation of the histograms of relative frequency a non-overlapping sliding time window of $W = 100$ points is adopted, producing a total of $k = 1, \cdots, 70$ samples.
- In the genomic series (human chromosome Y) we have:
  - Four bases denoted {A,C,T,G} that are sampled in groups of 3 producing histograms with 4^3 bins.
  - A small percentage of triplets involving the symbol N (considered as "not useful" in genomics) are not analysed.
  - A sequence of size $L = 872 \cdot 10^4$ is adopted and a non-overlapping sliding window of $W_2 = 124571$ points is considered producing a total of $k = 1, \cdots, 70$ samples.

S_α versus (α, k), $-1 \le \alpha \le 1$:
Dow Jones Industrial Average time series, Human chromosome Y

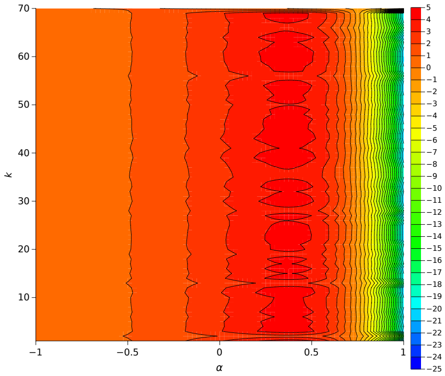

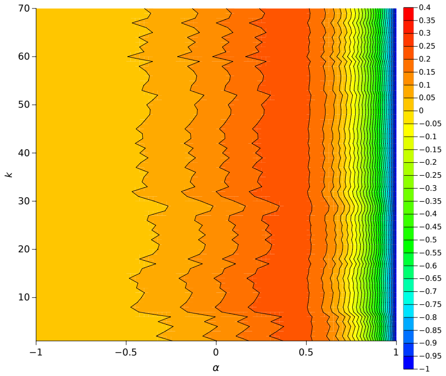

Jensen-Shannon divergence

The Kullback-Leibler and Jensen-Shannon divergence of Q from P:

$$D_{KL}\left(P \parallel Q\right) = \sum_i p_i \ln \frac{p_i}{q_i} \tag{23}$$

$$JSD\left(P \parallel Q\right) = \frac{1}{2}\left[D_{KL}\left(P \parallel M\right) + D_{KL}\left(P \parallel M\right)\right] \tag{24}$$

where $M = \frac{P+Q}{2}$. Therefore, the JSD can be generalized to:

$$\begin{aligned} JSD_\alpha\left(P \parallel Q\right) = {} & \frac{1}{2}\sum_i p_i \left\{-\frac{p_i^{-\alpha}}{\Gamma\left(\alpha+1\right)}\left[\ln p_i + \psi\left(1\right) - \psi\left(1-\alpha\right)\right]\right\} + \\ & \frac{1}{2}\sum_i q_i \left\{-\frac{q_i^{-\alpha}}{\Gamma\left(\alpha+1\right)}\left[\ln q_i + \psi\left(1\right) - \psi\left(1-\alpha\right)\right]\right\} \\ & - \sum_i m_i \left\{-\frac{m_i^{-\alpha}}{\Gamma\left(\alpha+1\right)}\left[\ln m_i + \psi\left(1\right) - \psi\left(1-\alpha\right)\right]\right\} \end{aligned} \tag{25}$$

Application of the JSD_α to human chromosomes

We consider the set of $n = 24$ human chromosomes labeled as $\{$Hu1, ..., Hu22, HuX, HuY$\}$

- The chromosome bases are read in triplets feeding 4^3 bins of histograms of relative frequency of occurrence
- A comparison $n \times n$ symmetrical matrix **D** of element to element relative distances is constructed
- The results are visualized by means of Phylip (plots using options "neighbor" and "drawtree"), a package of programs for inferring phylogenies
- The algorithms produces a tree based on matrix **D**, trying to accommodate the distances into the two dimensional space

Phylip with algorithm “neighbor” and visualization by “drawtree” of the 24 human chromosomes compared by means of I_α, $\alpha = 0.5$

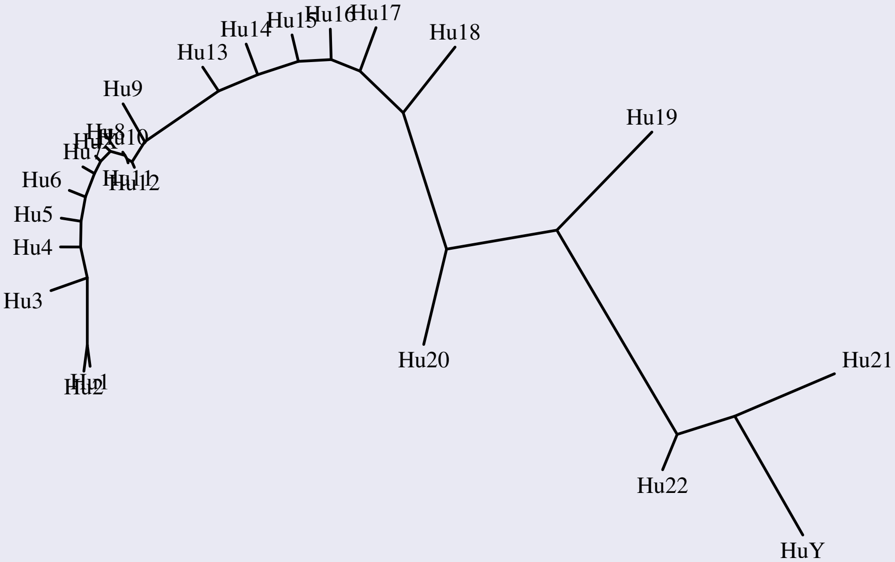

Visualization of dynamics

- António M. Lopes, J. A. Tenreiro Machado, Dynamics of the *N*-link pendulum: A fractional perspective, International Journal of Control, 2016.
- António Mendes Lopes, José Tenreiro Machado, Visualizing Control Systems Performance: A fractional perspective, Advances in Mechanical Engineering, vol. 7, issue 11, pp. 1-8, 2015.

Dynamics of the *N*-link pendulum

$$\frac{d}{dt}\frac{\partial L}{\partial \dot{\theta}_k} - \frac{\partial L}{\partial \theta_k} = T_k \tag{26a}$$

$$L = K - P \tag{26b}$$

$$\mathbf{I}(\theta)\ddot{\theta} + \mathbf{N}(\theta, \dot{\theta}) + \mathbf{G}(\theta) = \mathbf{T} \tag{27}$$

N-link pendulum

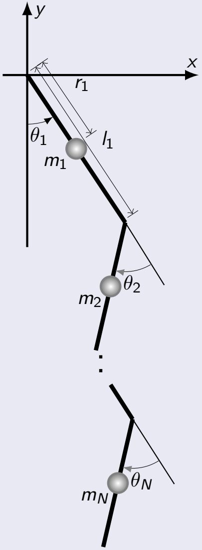

Pendulum direct dynamics

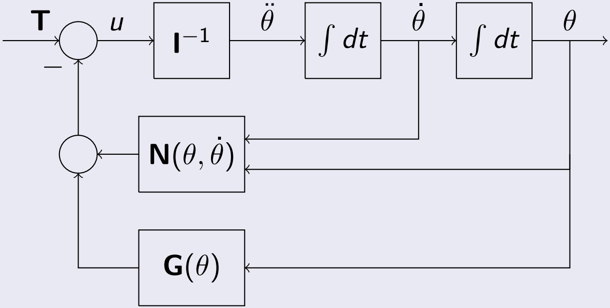

Traveling signal

- $\vartheta = (\mathbf{I}^{-1})^p \cdot \mathbf{u},\ p \in [0, 1],\ \mathbf{u} \Rightarrow \ddot{\theta}$
- $\psi = {}_aD_t^\alpha\, \ddot{\theta}(t),\ \alpha \in [-2, 0],\ \ddot{\theta} \Rightarrow \theta$

Forward signal propagation for the 1-link planar pendulum: ϑ_1, ψ_1

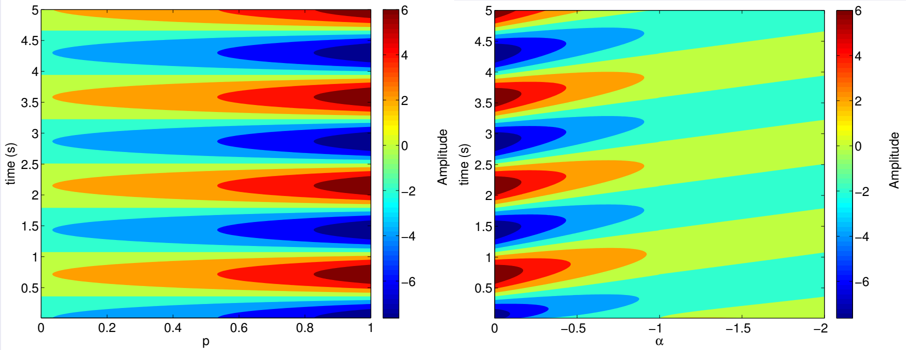

Forward signal propagation for the 2-link planar pendulum: ϑ_1, ψ_1

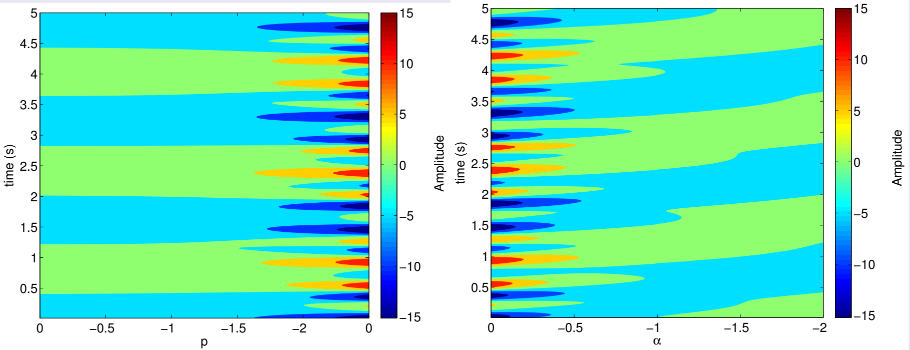

Forward signal propagation for the 3-link planar pendulum: ϑ_1, ψ_1

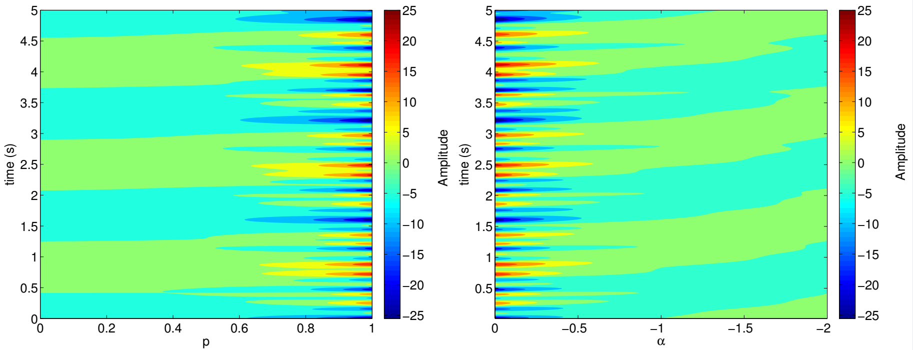

Modelling vegetables

- António M. Lopes, J. A. Tenreiro Machado, Fractional Order Models of Leaves, J. of Vibration and Control, vol. 20, No. 7, pp. 998-1008, 2014.
- António M. Lopes, J.A. Tenreiro Machado, Modelling Vegetable Fractals by means of Fractional-order Equations, Journal of Vibration and Control, vol. 22, issue 8, pp. 2100-2108, 2016

- Biological tissues are complex systems characterized by dynamic processes that occur at different lengths and time scales
- Leaves are most responsible for food production in vascular plants
- The study of individual leaves can reveal important characteristics of the whole plant, namely the nutrient concentration, the presence of diseases, tissue damage and rooting ability

Electrical impedance spectroscopy (EIS)

- EIS measures the electrical impedance of a specimen across a given range of frequencies, producing a spectrum that represents the variation of the impedance versus frequency
- It involves exciting the specimen under study by means of electric sinusoidal signals and registering the system response
- EIS has been used for studying biological tissues, while avoiding aggressive examinations

- Voltage and the current across the specimen are, in time domain: $v(t) = V\cos(\omega t + \theta_V)$, $i(t) = I\cos(\omega t + \theta_I)$
- In frequency-domain: $\mathbf{V}(j\omega) = V \cdot e^{j\theta_V}$, $\mathbf{I}(j\omega) = I \cdot e^{j\theta_I}$
- The complex impedance is: $\mathbf{Z}(j\omega) = \frac{\mathbf{V}(j\omega)}{\mathbf{I}(j\omega)} = |\mathbf{Z}(j\omega)| \cdot e^{j\arg[\mathbf{Z}(j\omega)]}$

Experimental setup

- The specimens are immersed in water at 15 °C, except their petiole
- Two 0.5 mm diameter copper electrodes are used
  - One electrode is 10 mm inserted into the leaf petiole
  - One electrode is placed immersed in the salted water
- An adaptation resistance, $R_s = 15\ \text{k}\Omega$, is used in series

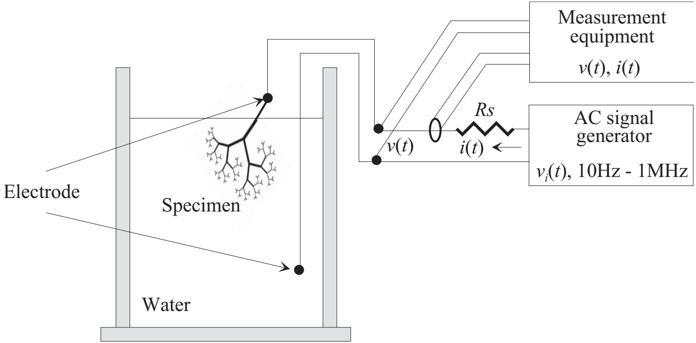

Methodology

- Experiments involve 3 different leaf samples of 2 distinct plants:
  - Bracken (*Pteridium aquilinum*)
  - Anthurium (*Anthurium andraeanum*)
  - Frequency range for EIS: 10 Hz $\leq f \leq$ 1 MHz, for $N = 30$ logarithmic spaced points

- Fitting:
  - Standard genetic algorithm, with elitism, crossover within all population and 5% mutation probability
  - Population of 6000 individuals, 6000 iterations
  - Fitness function:

$$J = \frac{1}{N} \sum_{k=1}^{N} \frac{\left[\Re_{exp}(\omega_k) - \Re_{mod}(\omega_k)\right]^2 + \left[\Im_{exp}(\omega_k) - \Im_{mod}(\omega_k)\right]^2}{\left[\Re_{exp}(\omega_k) + \Re_{mod}(\omega_k)\right]^2 + \left[\Im_{exp}(\omega_k) + \Im_{mod}(\omega_k)\right]^2}$$

Data analysis and results

- A good occurs for the Havriliak-Negami model: $G(j\omega) = \frac{K}{\left[1+\left(\frac{j\omega}{\omega_p}\right)^{\alpha}\right]^{\beta}}$
- The values
  - K and ω_p vary with the leaf size
  - α and β remain almost invariant

Leaf specimen		Area (mm^2)	K	ω_p	α	β	J
Bracken *Pteridium aquilinum*		22848	28395.56	30190.56	0.376	2.109	0.178
		14184	27929.71	43807.77	0.297	2.551	0.142
		4857	19839.88	267357.11	0.432	2.456	0.326
Anthurium *Anthurium andraeanum*	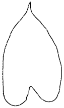	11591	122965.77	1742.80	0.558	1.296	0.191
		4878	101670.76	2957.08	0.593	1.314	0.271
		2281	71862.53	3350.45	0.593	1.314	0.415

Polar plots

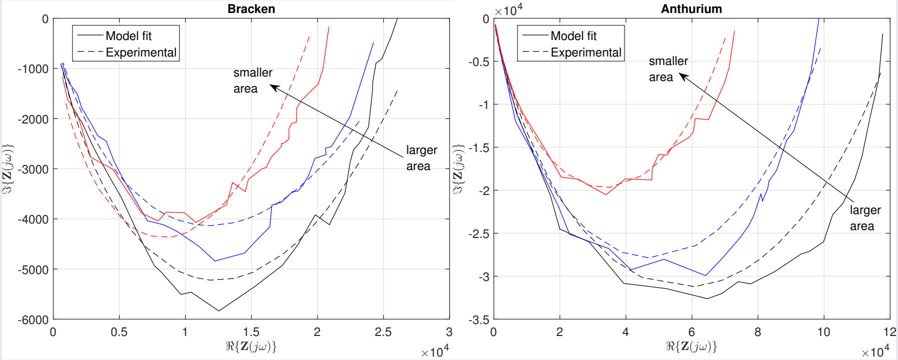

Bracken
Model fit
Experimental
smaller area
larger area
ℜ{Z(jω)}
ℑ{Z(jω)}
×10^4
Anthurium
Model fit
Experimental
smaller area
larger area
ℜ{Z(jω)}
ℑ{Z(jω)}
×10^4

Analyzing terrorism

- António M. Lopes and J. A. Tenreiro Machado, Analysis of Terrorism Data-series by means of Power Law and Pseudo Phase Plane, Discontinuity, Nonlinearity, and Complexity, vol. 4, n. 4, pp. 403-411, 2015
- António Mendes Lopes, José Tenreiro Machado, Maria Eugénia Mata, Analysis of global terrorism dynamics by means of entropy and state space portrait, Nonlinear Dynamics, vol. 85, Issue 3, pp. 1547-1560, 2016

- It is studied the global terrorism dynamics over the period 1970-2014.
- Data about terrorist events are analyzed by means of fractal dimension, entropy and multidimensional scaling
- The tools reflect the dynamics in time and space.

Total number of terrorist events per year, during the period 1970-2014

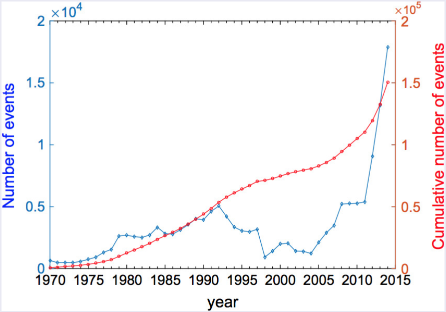

Geographic distribution of worldwide terrorist events during the period 1970-2014

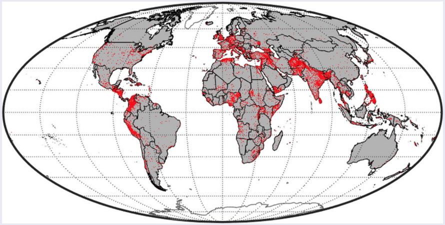

Relationship between the fractal dimension, b, and the Boltzmann-Gibbs-Shannon, S, and fractional, S^α, entropies, during the period 1970-2014

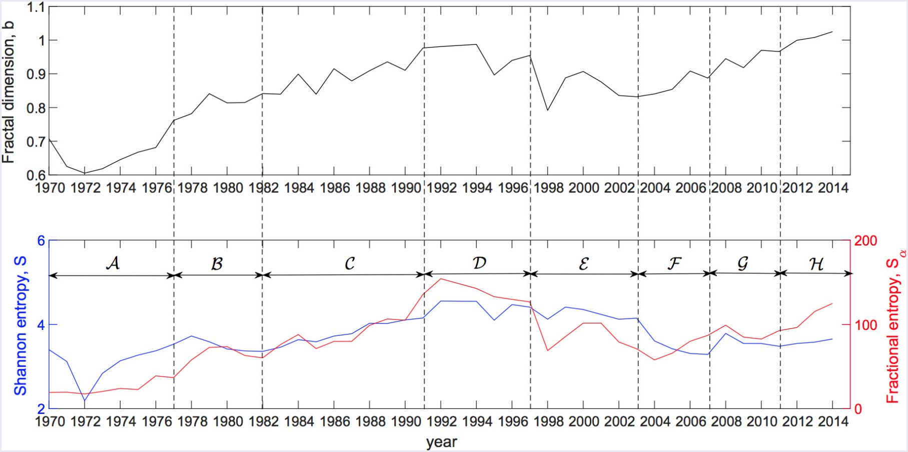

Tree generated by the HC algorithm, comparing the spacial statistical distributions of terrorist events, during the period 1970-2014, by means of the Jensen-Shannon divergence, $JSD^{\alpha}(P \parallel Q)$, $\alpha = 0.7$

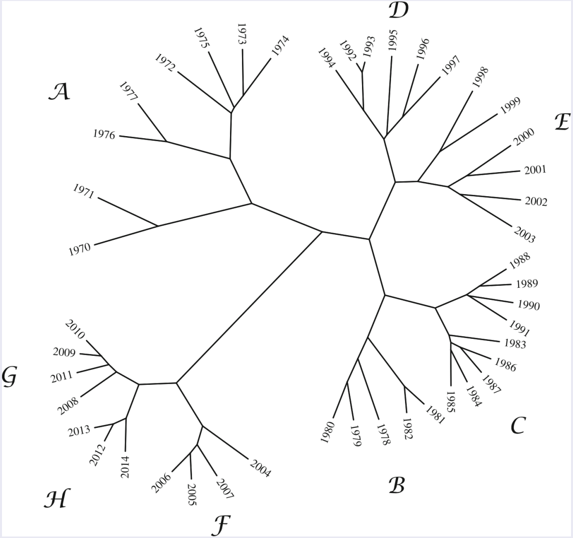

Map generated by the MDS and the superimposed pathway, comparing the spacial statistical distributions of terrorist events, during the period 1970-2014, by means of the Jensen-Shannon divergence, JSD^{α} (P ∥ Q), $\alpha = 0.7$

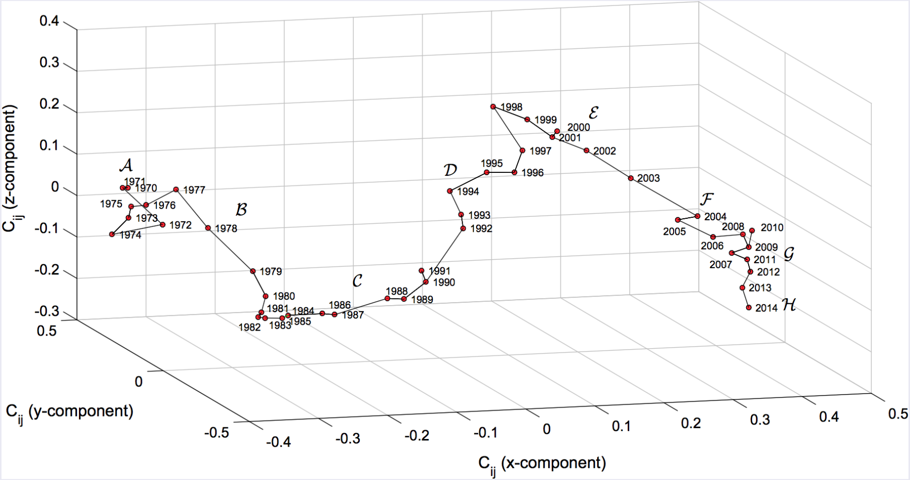

The most incomprehensible thing about the world is that it is at all comprehensible

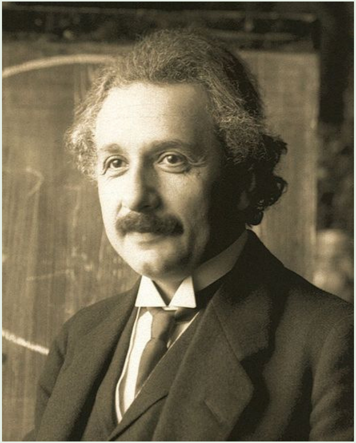

Popular strange things